Journal of
Synchrotron
Radiation

ISSN 0909-0495

Received 13 November 2003
Accepted 21 October 2004

Theory of Ca $L_{2,3}$-edge XAS using a novel multi-channel multiple-scattering method

Peter Krüger[a]* and Calogero R. Natoli[b]

[a]LRRS, UMR 5613 Université de Bourgogne, CNRS, BP 47870, 21078 Dijon, France, and [b]INFN Laboratori Nazionali di Frascati, Casella Postale 13, 00044 Frascati, Italy.
E-mail: peter.kruger@u-bourgogne.fr

A new method for calculating X-ray absorption spectroscopy (XAS) at the $L_{2,3}$ edges of Ca and transition metals is presented. It is based on the multichannel multiple-scattering theory by Natoli *et al.* [*Phys. Rev. B*, (1990), **42**, 1944–1968] combined with the eigen-channel R-matrix formalism. Atomic multiplet-like effects, owing to the Coulomb interaction of photoelectrons and the 2*p* hole, are taken into account through a configuration interaction ansatz for the final-state wavefunction. The various multiplet states lead to a set of channels for the photoelectron wavefunction, which is calculated in multiple-scattering theory. The method is applied to Ca, an important element for biological applications of XAS. An $L_3{:}L_2$ branching ratio of 3:4 is found, in good agreement with experiment but in contrast to the statistical value 2:1 obtained in all one-electron approaches. By using a linear mixture between statically screened ($\sim$90%) and unscreened ($\sim$10%) core-hole potential, the line shape, too, agrees well with the experimental one.

Keywords: X-ray absorption fine structure; $L_{2,3}$-edges; calcium; multiple scattering; electron correlation.

1. Introduction

Many proteins interact strongly with certain heavy elements, which act as cofactors or as part of substrate binding/utilization sites. The number of such elements, however, is small; among them is Ca and most 3*d* transition-metal elements, like Zn, Fe, Mn, Cu, Ni, Co and Mo. The active site of such metalloproteins exhibits distinctive spectral features compared with small molecular inorganic complexes of the same metal ion. These features are the result of the unusual geometric and electronic structure that can be imposed on the metal ion in a protein environment. The detailed investigation of the electronic and structural properties of the metal site is fundamental for the understanding of the function of these macromolecules, the mechanism of the catalytic processes and the stability of the protein.

To this purpose, X-ray absorption spectroscopy (XAS) has proved to be an invaluable tool in the study of the chemical and structural properties of biological systems, owing to its atomic selectivity and the possibility of carrying out measurements at very low concentration and in any physical state (aqueous and crystalline). In this respect the low-energy part of the metal *K*-edge spectra has been found to be extremely sensitive to the structural details of the absorbing site, like overall symmetry, distances and bonding angles, and substantial progress has recently been made in the theoretical simulations of the near-edge part of the spectrum in order to obtain this kind of information (Natoli *et al.*, 2003; Benfatto *et al.*, 2003). *K*-edge spectra are also sensitive to oxidation state, valence and spin state, but in a less direct way, which makes the theoretical interpretation more difficult and less efficient. XAS at the $L_{2,3}$ edges, on the other hand, is highly sensitive to these properties, since they are mainly carried by the 3*d* states, which are directly probed at these absorption edges. Thus, a quantitative analysis of the $L_{2,3}$-edge XAS would provide important complementary information to the *K*-edge XAS.

So far, the $L_{2,3}$ edges have largely been neglected for biological applications of XAS, which is probably due to the theoretical difficulties in the modelization of these spectra. The strong 2*p*–3*d* Coulomb and exchange interaction leads to a multiplet structure that cannot be reproduced within the independent-particle approximation, but requires the use of some many-body theory. The failure of the independent-particle picture is most easily recognized in the $L_{2,3}$-edge branching ratio problem: the experimental branching ratio, *i.e.* the intensity ratio between the L_3 and L_2 'white' lines, is roughly 1:1 in Ca and the light transition elements, while the independent-particle approximation yields 2:1 (Zaanen *et al.*, 1985). This large deviation is due to the Coulomb and exchange interaction of the 2*p* hole with the 3*d* electrons in

the final state, which, together with the rather small $2p$ spin–orbit coupling, leads to a strong configuration mixing between $2p_{3/2}$ and $2p_{1/2}$ hole states.

This correlation effect can easily be handled in the case of isolated atoms by using standard atomic multiplet theory (Condon & Shortley, 1951); consequently, $L_{2,3}$ XAS spectra calculated within atomic multiplet theory have branching ratios in good agreement with experiment (de Groot *et al.*, 1990). However, the atomic models have the major shortcoming that all extra-atomic effects, such as band formation and ligand field splitting, can only be described in an empirical way by introducing a set of adjustable parameters. An example of this kind of analysis, which can nonetheless lead to useful comparative understanding of the electronic structure of the metal site in different environments, was given by van Elp *et al.* (1994).

The atomic model approaches are quite unsatisfactory for the XAS experimentalists, who are mainly interested in the extra-atomic effects on the spectra and who need predictive theoretical methods for an independent comparison with the experimental results. A predictive method should rely on a first-principle calculation of the electronic structure of the extended system, but should still include local electron correlation effects of the atomic multiplet type. Such a method is still lacking. However, some promising progress in the branching-ratio problem has been achieved by different authors. In a pioneering work, Zaanen *et al.* (1985) combined band-structure effects and the photoelectron–core-hole Coulomb interaction using a two-particle Green's function method. The approach yielded good results but had strong model character: it used atomic orbitals and model density of states. Much later, Schwitalla & Ebert (1998) presented the first first-principle calculation by using a time-dependent local density approximation (TDLDA). While good results were obtained for the branching ratio of Ca and the light $3d$ elements, several problems remained: the line shape of Ca XAS, for example, was very different from experiment, and the branching ratio of the heavier elements was worse than that obtained in the independent-particle approximation. The latter problem was very recently solved by Ankudinov *et al.* (2003), who improved Schwitalla's approach by adding dynamical screening corrections, partly based on the Bethe–Salpether equation, to the TDLDA.

Here we present a very different and, we believe, more intuitive approach, which is based on the multichannel multiple-scattering (MS) formalism developed by Natoli *et al.* (1990) and the atomic R-matrix theory (Hamacher & Hinze, 1989; Aymar *et al.*, 1996). The formalism is briefly outlined in the next section, followed by an application to the $L_{2,3}$-edge XAS of bulk Ca metal.

2. Formalism

In the X-ray absorption process at the $L_{2,3}$ edges, an electron is excited from the $2p$ core level to a continuum state above the Fermi level. We consider the six-electron wavefunction made of the $2p$ core electrons, one of which becomes the photoelectron in the final state. All other electrons are not considered explicitly; they are assumed to contribute only to the mean-field potential. The initial state Ψ_g with energy E_g is simply given by the closed-shell configuration $(2p^6, {}^1S_0)$. Final states have energy $E = E_g + \hbar\omega$ and a $(2p^5\varepsilon^1)$ configuration, where ε denotes a (one-electron) state in the continuum above the Fermi energy. Following Natoli *et al.* (1990), we use a configuration interaction ansatz for the final-state wavefunction, which is developed as

$$\Psi = \mathcal{A} \sum_{\beta} \tilde{\Phi}_{\beta}(X)\varphi_{\beta}(x). \tag{1}$$

Here $\tilde{\Phi}_{\beta}$ is one of the six $(2p^5)$ states, labelled by $\beta = (j_c, \mu_c)$ ($j_c = 1/2, 3/2$, $\mu_c = -j_c \ldots j_c$); X collects all core-electron coordinates. For each $\tilde{\Phi}_{\beta}$, there is a component φ_{β} of the photoelectron wavefunction. The (radial, angular and spin) coordinate of the photoelectron is denoted $x = (r, \hat{x}, \sigma)$. Finally, $\mathcal{A}$ denotes the antisymmetrization operator.

For correlated N-electron wavefunctions such as Ψ in (1), where all electrons but one occupy localized orbitals, we have derived a multichannel MS method for XAS in close formal analogy to the standard single-electron method (Krüger & Natoli, 2004). The total photoabsorption cross section is given by Natoli *et al.* (1990) and Krüger & Natoli (2004),

$$\sigma(\omega) \propto \omega\, \mathrm{Im}\left(\sum_{\Gamma\Gamma'} M_{\Gamma}^{*}\, \tau_{\Gamma\Gamma'}^{00}\, M_{\Gamma'} \right). \tag{2}$$

Here $\Gamma = \beta lms$ is the set of all quantum numbers of Ψ, with lms being the orbital and spin quantum numbers of the photoelectron. Each different Γ is called a channel. $M_{\Gamma} = \langle \Psi_{\Gamma}^{\mathrm{in}} | D | g \rangle$ is a dipole transition matrix element and $\Psi_{\Gamma}^{\mathrm{in}}$ is the wavefunction inside the atomic sphere that matches smoothly onto the outside solution. Further, $\tau_{\Gamma\Gamma'}^{ij}$ is the multichannel scattering path operator connecting sites i and j. It is calculated for a finite cluster by inversion of the τ^{-1} matrix, whose elements are given by

$$[\tau^{-1}]_{\Gamma\Gamma'}^{ij} = \delta_{ij}[t^{-1}]_{\Gamma\Gamma'}^{i} - \delta_{\beta\beta'}\, k_{\beta}\, H_{lm,l'm'}^{ij}(k_{\beta})\, \delta_{ss'}. \tag{3}$$

Here, t^i is the (multichannel) atomic T-matrix of atom i, and $H_{lm,l'm'}^{ij}$ are the real-space KKR structure factors [for a definition, see Appendix A of Natoli *et al.* (1990)]. k_{β} is the wavenumber of the photoelectron, given by $k_{\beta}^2 + V_0 = \varepsilon_{\beta} = E - E_{\beta}$, where V_0 is the interstitial potential and E_{β} is the excitation energy of state β. We take into account only local electron correlation effects on the absorbing atom ($i = 0$). Therefore, only the T-matrix of atom $i = 0$ has a multichannel structure: $t_{\Gamma\Gamma'}^{i} = \delta_{\Gamma\Gamma'} t_{l}^{i}$ for all $i \neq 0$. For the results shown below we have used a symmetric f.c.c. cluster up to the tenth neighbor shell (177 atoms) with t^i-matrices ($i \neq 0$) obtained from self-consistent linear-muffin-tin-orbital (LMTO) potentials (Andersen & Jepsen, 1984) within the local density approximation (LDA).

The above formulae are very similar to those of standard MS theory except that the absorber's T-matrix and dipole matrix elements are multichannel quantities that have to be evaluated with the correlated wavefunction Ψ rather than with

single-electron wave functions. Ψ can be obtained by solving a set of coupled integro-differential Schrödinger-type equations which are coupled by the multichannel potential (see Natoli *et al.*, 1990). Here we follow another route which avoids the difficult calculation of the multichannel potential. Instead, we used the eigen-channel R-matrix method, which allows a variational calculation of the atomic multichannel T-matrix and the inner solutions $\Psi^{\rm in}$. It requires the confinement of all but one electronic orbitals in the atomic volume, which is justified for our choice of Ψ. For details on the eigen-channel method, the reader is referred to the standard literature (Aymar *et al.*, 1996; Hamacher & Hinze, 1989).

The physical meaning of this multichannel MS theory is quite simple and can be read off from (2). In one-electron MS theory, which is a one-channel problem, the absorption cross section is proportional to the imaginary part of the probability amplitude that the ejected photoelectron emitted by the photoabsorber returns thereon after being scattered by the surrounding. In practice, the photoabsorber acts as a source of electrons as well as a detector. As is well known, this quantity is the projected density of states of the system at the photoelectron energy onto the central photoabsorbing atom. In the multichannel version, where the dynamical response of the system is limited to the photoabsorber, the photoelectron can exchange energy with the central atom in its way out to the system and back, jumping from one channel to another, *i.e.* exciting the various $2p$–$3d$ multiplets in the case at hand. The imaginary part of the scattering amplitudes for all these processes constitute a sort of generalized density of states, to which the absorption cross section is proportional. In this way, weight is transferred from the $j_c = 3/2$ channel to the $j_c = 1/2$ channel.

In the practical implementation of the theory, we describe the electronic system by the Hamiltonian $H = h + V$, where h stands for the single-electron part with the 'best' effective potential and V is the residual electron–electron interaction. As 'best' effective potential in the final state, we use a linear mixture between a statically screened core-hole potential and an unscreened one,

$$v(r) = (1 - \alpha)\, v_s(r) + \alpha v_u(r),$$

where α is a mixing parameter. The screened part v_s is obtained from a self-consistent LDA-LMTO calculation for a 32-atom supercell with a $2p$ core-hole at the absorber site. The unscreened part v_u is given by the sum of the ground-state potential (no hole relaxation) and the Hartree potential of a spherically symmetric $2p$ hole. This Hartree potential corresponds to the monopole term $2/r_>$ of the bare Coulomb interaction operator $2/|r - r'|$. Therefore the residual Coulomb interaction is given by $V = 2/|r - r'| - 2/r_>$. Note that this amounts to taking a simple screening model for the monopole part of the electron–hole Coulomb interaction (linear mixture between unscreened and statically screened terms), while all higher-order multipole and exchange terms are left unscreened.

As trial states of the eigen-channel method we use the functions

$$\Psi_{\Gamma\nu} \equiv \mathcal{A}\big[\Phi_\Gamma(X\hat{x}\sigma)P_\nu(r)/r\big]. \quad (4)$$

Here, $\Phi_\Gamma(X\hat{x}\sigma) \equiv \tilde{\Phi}_\beta(X)Y_{lm}(\hat{x})\delta_{s\sigma}$, where Y_{lm} is a spherical harmonic. For P_ν, we take solutions of the radial Schrödinger equation for angular momentum l with the effective potential v. Since $2p \rightarrow \varepsilon s$ transitions have negligible intensity in the near-edge region, we here include only $l = 2$, *i.e.* d-waves in the basis. We use closed-type orbitals with boundary conditions $P_\nu(r_0) = 0$, and open-type orbitals with boundary conditions $\mathrm{d}P_\nu/\mathrm{d}r(r_0) = 0$. Here, r_0 is the radius of the atomic sphere. Convergence of the spectra was achieved with five closed-type orbitals (with zero to four nodes in $0 < r < r_0$) and one open-type orbital (with zero nodes). The only non-trivial matrix elements to be calculated for the eigen-channel method are those of V. The Coulomb interaction $2/|r - r'|$ can be expressed in terms of (generalized) Slater integrals $F^k_{\nu\nu'} \equiv (2p, \nu d|r^k/r^{k+1}|2p, \nu' d)$ and $G^k_{\nu\nu'} \equiv (2p, \nu d|r^k/r^{k+1}|\nu' d, 2p)$ like in atomic theory (Condon & Shortley, 1951). Subtraction of the monopole term $2/r_>$ simply makes all F^0 terms vanish, while leaving all other terms unchanged.

3. Results and discussion

For better understanding of the results, we first consider the independent-particle approximation, *i.e.* we set the residual Coulomb interaction V to zero. The lower two spectra of Fig. 1 have been calculated for $V = 0$ and the screening parameter $\alpha = 0$ and $\alpha = 0.1$, respectively. The value $\alpha = 0$ corresponds to the statically screened core-hole approximation, which is often used in calculations for K-edge XAS. One can recognize the slightly overlapping L_3- and L_2-edge parts with energy ranges

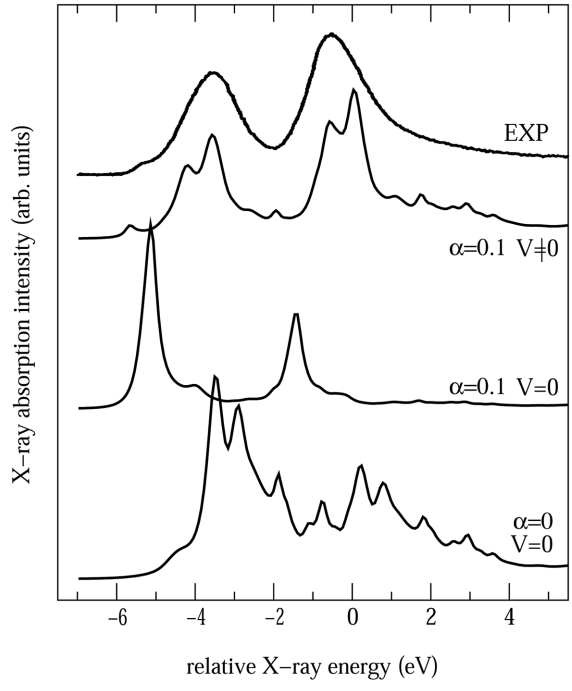

Figure 1
X-ray absorption spectra at the $L_{2,3}$-edge of Ca metal calculated within different approximations (see text) along with the experimental results (EXP).

roughly from −4 to 0 eV and from −0.5 to 3.5 eV. The branching ratio is about 2:1, as expected for the independent-particle approximation. Comparison of this spectrum with that obtained with $V = 0$ and $\alpha = 0.1$ shows the effect of increasing α; we recall that α is the fraction of the unscreened part (sum of ground-state potential plus Hartree potential of the core hole) in the one-electron final-state potential for the photoelectron wavefunction. It can be seen that increasing α makes the spectrum quickly tend to the free-atom-like shape, which has a simple two-peak structure (for $V = 0$). Increasing α makes the potential more attractive such that the *d*-resonance falls below the (*d*-like) conduction band. As a consequence, MS becomes impossible and the photoelectron becomes confined to the atom. Needless to say, the branching ratio is not affected by the change of α. It does change dramatically, however, upon 'switching' on V, as can be seen from comparison with the uppermost theoretical spectrum in Fig. 1 (labelled '$\alpha = 0.1, V \neq 0$'). The branching ratio is about 3:4 and is thus in good agreement with the experimental value (see the experimental spectrum, labelled 'EXP').

The spectra shown in Fig. 2 have been calculated including V, and for different values of α. For $\alpha = 0$ the spectrum consists of a single 7 eV-wide broad feature with small variations of the amplitude. The line shape is very different from the experimental one with its simple two-peak structure (plus a very small shoulder at the low-energy side). The spectra with $\alpha = 0.1$ or $\alpha = 0.15$ resemble much more the experimental one. The peak widths and relative intensities are in good agreement with experiment. The only disagreement is that the theoretical curves display some fine structure (owing to MS in the solid) which is absent in the experimental spectrum. This may be mainly due to core-hole decay processes, in particular a strong auto-ionization as proposed by Himpsel *et al.* (1991). It could, however, also reveal limitations of our static screening model for the one-electron potential v.

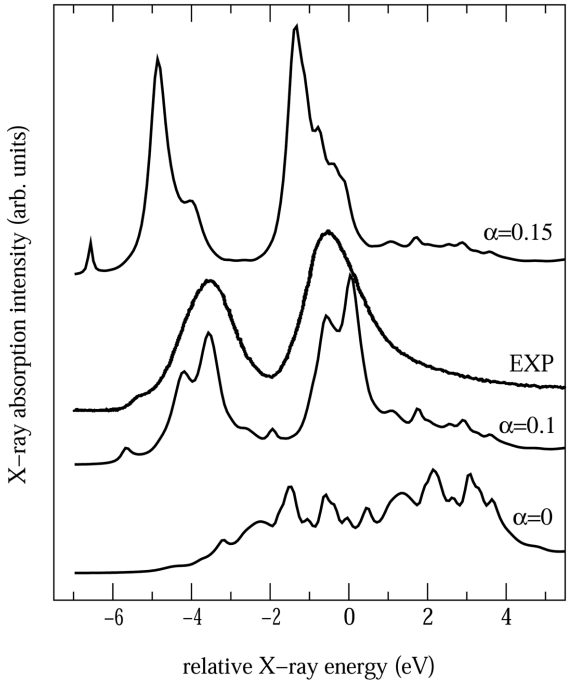

Figure 2
Same as Fig. 1 except that $V \neq 0$ (*i.e.* the residual Coulomb interaction has been taken into account) in all cases.

4. Conclusions

In summary, we have presented a new method for XAS calculations that combines the multichannel multiple-scattering formalism and the eigen-channel R-matrix method. The method features an *N*-electron configuration interaction calculation for the absorbing atom and thus takes account of atomic multiplet-like effects. Unlike atomic models, however, the photoelectron wavefunction is delocalized and thus strongly influenced by multiple-scattering events from the whole system. We have applied the method to the $L_{2,3}$ edge of Ca, an important element for biological applications of XAS. While all calculations within the independent-particle approximation yield an $L_3:L_2$ branching ratio of about 2:1, we obtain a value of about 3:4, in good agreement with experiment. We have treated screening of the monopole Coulomb interaction within a simple model, namely a linear mixing of the statically screened core-hole potential and the unscreened Hartree potential of the core hole. Potentials with 10–15% unscreened part yield line shapes in good agreement with experiment.

The approach presented above combines, in a simple way, the accuracy of the one-particle description of the system based on the multiple-scattering theory with a realistic formulation of the dynamical scattering of the photoelectron with the photoabsorber. As apparent from Natoli *et al.* (1990) and Krüger & Natoli (2004), one can take into account with little more effort the dynamical response not only of the central atom but also of the nearest neighbours in the frame of the R-matrix formulation of the scattering problem. We are rather confident that this method will in the future constitute the basis for a quantitative investigation of the *L* edges of the metal centres in proteins and will provide valuable information on their electronic properties, like oxidation state, spin state and chemical binding.

The main part of this work was carried out while PK was under contract at the European Synchrotron Radiation Facility, Grenoble, France.

References

Andersen, O. K. & Jepsen, O. (1984). *Phys. Rev. Lett.* **53**, 2571–2574.
Ankudinov, A. L., Nesvizhskii, A. I. & Rehr, J. J. (2003). *Phys. Rev. B*, **67**, 115120.
Aymar, M., Greene, C. H. & Luc-Koenig, E. (1996). *Rev. Mod. Phys.* **68**, 1015–1123.
Benfatto, M., Della Longa, S. & Natoli, C. R. (2003). *J. Synchrotron Rad.* **10**, 51–57.
Condon, E. U. & Shortley, G. H. (1951). *The Theory of Atomic Spectra.* Cambridge University Press.
Elp, J. van, Peng, G., Searle, B. G., Mitra-Kitley, S., Johnson, M. K., Zhou, Z. H., Adams, M. W. W., Maroney, M. J. & Cramer, S. P. (1994). *J. Am. Chem. Soc.* **116**, 1918–1923.

Groot, F. M. F. de, Fuggle, J. C., Thole, B. T. & Sawatzky, G. A. (1990). *Phys. Rev. B*, **42**, 5459–5468.
Hamacher, P. & Hinze, J. (1989). *J. Phys. B*, **22**, 3397–3410.
Himpsel, F. J., Karlsson, U. O., McLean, A. B., Terminello, L. J., de Groot, F. M. F., Abbate, M., Fuggle, J. C., Yarmoff, J. A., Thole, B. T. & Sawatzky, G. A. (1991). *Phys. Rev. B*, **43**, 6899–6907.
Krüger, P. & Natoli, C. R. (2004). *Phys. Rev. B*, **70** In the press.
Natoli, C. R., Benfatto, M., Brouder, C., López, M. F. R. & Foulis, D. L. (1990). *Phys. Rev. B*, **42**, 1944–1968.
Natoli, C. R., Benfatto, M., Della Longa S. & Hatada, K. (2003). *J. Synchrotron Rad.* **10**, 26–42.
Schwitalla, J. & Ebert, H. (1998). *Phys. Rev. Lett.* **80**, 4586–4589.
Zaanen, J., Sawatzky, G. A., Fink, J., Speier, W. & Fuggle, J. C. (1985). *Phys. Rev. B*, **32**, 4905–4913.